Vol. 698: 29–39, 2022
doi: 10.3354/meps14153

MARINE ECOLOGY PROGRESS SERIES
Mar Ecol Prog Ser

Published October 6

Pneumatophores and crab burrows increase CO_2 and CH_4 emission from sediments in two Brazilian fringe mangrove forests

Erik Kristensen[1,*], Thomas Valdemarsen[1], Paula C. de Moraes[2], Arthur Z. Güth[2], Paulo Y. G. Sumida[2], Cintia O. Quintana[1]

[1]Department of Biology, University of Southern Denmark, Campusvej 55, Odense M 5230, Denmark
[2]Instituto Oceanográfico da Universidade de São Paulo, Praça do Oceanográfico, 191, Cidade Universitária, 05508-120 São Paulo, Brazil

ABSTRACT: We assessed the release of greenhouse gases (CO_2 and CH_4) from air-exposed sediments and dissolved inorganic carbon (DIC) from inundated sediments in 2 Brazilian mangrove forests. Our focus was on the impact of biogenic structures, i.e. pneumatophores and crab burrows, on greenhouse gas emissions. Emission of CO_2 from air-exposed bare sediment (111–156 and 57–148 mmol m^{-2} d^{-1} in darkness and in light, respectively) was comparable to DIC release from inundated sediment (122–158 and 52–62 mmol m^{-2} d^{-1}, respectively). Pneumatophores and crab burrows increased dark CO_2 emission during air exposure by 113–123 and 49–91%, respectively. CH_4 emission from air-exposed bare sediment (0.22–0.25 mmol m^{-2} d^{-1}) was increased 92–137 and 288–607%, respectively, by pneumatophores and burrows. Carbon loss in the form of CO_2 and DIC from sediments with biogenic structures can at the two study locations be extrapolated to 64.1 and 71.0 mol C m^{-2} yr^{-1}. These values fit well with literature values of litterfall in the studied area, providing carbon accretion of 28.5 and 21.6 mol C m^{-2} yr^{-1}. However, the budget will be unbalanced if the role of biogenic structures is not considered. In the presence of biogenic structures, CH_4 emissions of 2.8 and 3.3 mol C m^{-2} yr^{-1} (when converted to CO_2 units) will partly (10–15%) counteract the climate mitigation effect of the accumulated carbon. Carbon budgets in mangrove sediments may therefore be flawed if the contribution of biogenic structures to greenhouse gas emissions is ignored.

KEY WORDS: Greenhouse gas emission · Biogenic structures · Climate mitigation · Blue carbon

1. INTRODUCTION

Mangrove forests are considered important blue carbon ecosystems with a high capacity to sequester and store carbon (C) in anoxic sediments and thus mitigate global climate change (Alongi 2012, Jennerjahn 2020). Together with saltmarshes and seagrass beds, mangrove forests are responsible for a disproportionally large fraction of the marine blue carbon storage, despite the relatively small areal coverage of these ecosystems (Kristensen et al. 2017, Macreadie et al. 2021, Wang et al. 2021). Mangrove forests are largely restricted to tropical and subtropical areas, where they cover a total of only 130 000–150 000 km^2 (Giri et al. 2011, Spalding et al. 2011, Friess et al. 2019). The mangrove area in Brazil is estimated to be about 10% of the global coverage and extends along more than 90% of the coastline (Spalding et al. 2011, Schaeffer-Novelli et al. 2016).

C inputs to mangrove sediments are dominated by primary production of mangrove trees and import of organic and inorganic particles from upstream rivers and the coastal ocean (Matos et al. 2020, Sasmito et al. 2020). Conversely, C losses occur through respira-

*Corresponding author: ebk@biology.sdu.dk

Publisher: Inter-Research · www.int-res.com

tion by trees, benthic fauna and microbial decomposers, as well as carbonate dissolution combined with emission of gases to the atmosphere and tidal export of solutes and particles (Alongi 2020a). A global average balance between these sources and sinks of C reveals that mangrove forests have the potential to accumulate and sequester around 170 g C m^{-2} yr^{-1} (Pérez et al. 2018, Alongi 2020b). However, there are still gaps in mangrove C budgets, since measured sinks such as burial, CO_2 emission and tidal export in many cases cannot fully balance the estimated C sources in the form of primary production and tidal import (Bouillon et al. 2008).

It has been suggested that the C budget deficiency of mangrove forests is caused by underestimated sinks in the form of excess emission of CO_2 via biogenic structures, such as pneumatophores, cable roots and crab burrows (Kristensen et al. 2008, Alongi 2020a). During low tide, these structures provide air-filled conduits from the sediment to the atmosphere driven by a diffusive transport that is 10 000 times faster than in sediment porewater (Kristensen et al. 2022). Although the contribution of pneumatophores and crab burrows to CO_2 emission into the atmosphere may increase the C loss, there is still room for substantial blue carbon formation in mangrove sediments (Alongi 2020b). In fact, these structures may instead close the gaps and complete mangrove C budgets.

There are indications, however, that the contribution of other greenhouse gases (CH_4 and N_2O) which are more potent than CO_2 may threaten the warming mitigation capacity of the accumulated blue carbon in mangrove forests (Rosentreter et al. 2021). For example, CH_4 has a global warming potential that is up to 34 times higher than CO_2 on a 100 yr scale when climate C feedbacks are included (Gillett & Matthews 2010, Myhre et al. 2013). In a recent review, Kristensen et al. (2022) found that the global warming mitigation of blue carbon in mangrove forests is offset to almost zero when including the effect of pneumatophores, cable roots and crab burrows as channels for rapid emission of CH_4 and N_2O.

The aim of the present study was to determine emissions of 2 greenhouse gases (CO_2 and CH_4) and the release of dissolved inorganic carbon (DIC) from sediments in 2 Brazilian fringe mangrove forests adjacent to and distant from the urban areas of Cananéia City. Focus was particularly on the influence of biogenic structures, i.e. pneumatophores and crab burrows, for the emission of CO_2 and CH_4 to the atmosphere. Gas emission during air exposure was determined using *in situ* techniques and during inundation using laboratory-based DIC exchange measurements. Based on the inundation frequency and duration during day and night over 1 mo, we quantified the total release of C-based greenhouse gases and compared it to known local estimates of C input. We used these results to assess the impact of biogenic structures on C budgets and the climate change mitigation potential of the explored Brazilian fringe mangrove forests.

2. MATERIALS AND METHODS

2.1. Study sites

The Cananéia Lagoon is a mangrove-surrounded estuary located near the southern border of São Paulo State, Brazil (Fig. 1). The estuary has 110 km^2 of water area (mean depth of 6.5 m) and is bordered by 72 km^2 of mangrove forest. It is connected to the South Atlantic Ocean by Cananéia Inlet in the south and Icapara Inlet in the north. Water exchange in the estuary is primarily the result of inflow of offshore water by tidal currents and outflow of fresh water from several rivers (Schaeffer-Novelli et al. 1990). The climate is mild subtropical, with average annual temperature ranging from 20°C in the dry winter (July to August) to 28°C in the wet summer (January to March); average annual precipitation is 2200 mm (Cunha-Lignon et al. 2009). The tidal regime is semidiurnal and microtidal, with average tidal amplitudes of 0.7 ± 0.3 m (mean ± SD).

The study was conducted during February 2014 in fringe mangrove forests adjacent to 2 creeks near the Cananéia Inlet. Olaria Creek is located close to Cananéia City on Cananéia Island, while Nobrega Creek is located on the unpopulated Comprida Island ca. 2 km away from Cananéia Island (Fig. 1). The mangrove forest surrounding Olaria Creek is periodically exposed to anthropogenic discharges from suburban parts of Cananéia City, while no such exposure occurs at Nobrega Creek (Aidar et al. 1997, Barcellos et al. 2005). The mangrove forest along both creeks is dominated by 3 mangrove species (*Laguncularia racemosa*, *Rhizophora mangle* and *Avicennia schauerianna*; Schaeffer-Novelli et al. 1990). The most abundant burrowing brachyuran crabs are *Ucides cordatus*, fiddler crabs (*Uca* spp.) and sesarmid crabs (e.g. *Aratus pisonii*).

Parallel samplings were conducted at comparable mangrove locations in Olaria (25.0204° S, 47.9294° W) and Nobrega (25.0137° S, 47.9133° W) Creeks. One intertidal location dominated by the mangrove

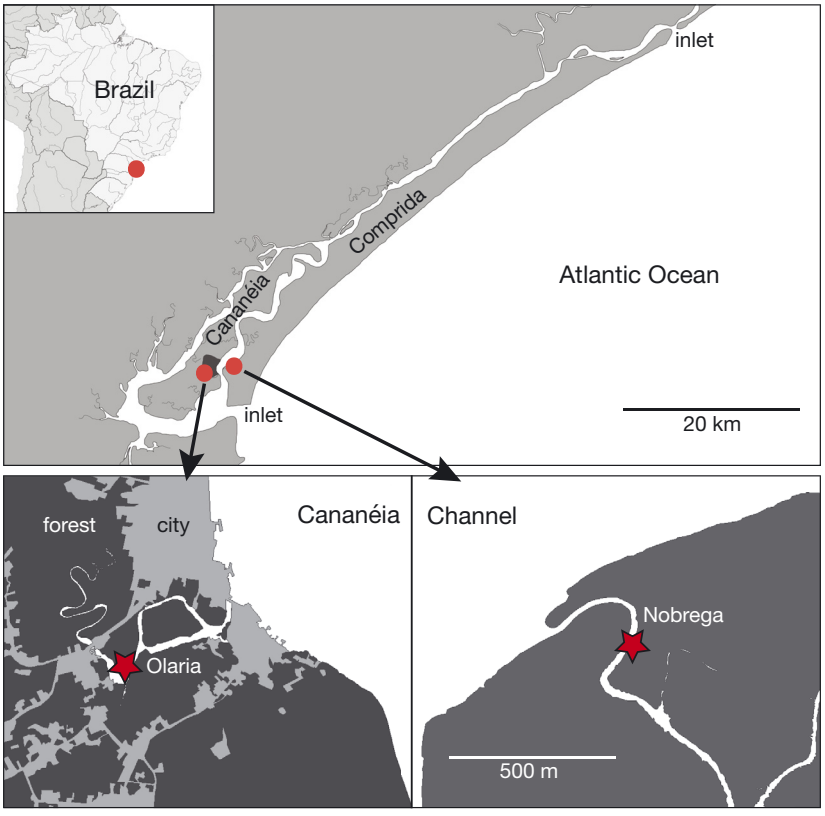

Fig. 1. Cananéia and Comprida Islands in Southern Brazil, showing Olaria Creek in the vicinity of Cananéia City on Cananéia Island and Nobrega Creek on Comprida Island. The study locations are indicated by stars

A. schauerianna was chosen 20 m inland of each creek with similar tidal elevation of the mangrove forest floor. The 2 locations were ~50 cm above mean sea level and were flooded 20–25 times monthly during high spring tides (Fig. 2). Salinity and water temperatures at both locations were 22.8–23.4 and 28–30°C at the time of sampling.

2.2. Density and size of pneumatophores and crab burrows

The density and size of visible biogenic structures (*A. schauerianna* pneumatophores and crab burrows) were determined from digital photographs taken of the mangrove forest floor simultaneously with the *in situ* incubations and sampling. Photographs at Olaria (n = 14) and Nobrega (n = 9), which included a known scale and covered on average 0.5 m^2 (range: 0.3–1 m^2) of the forest floor, were taken perpendicular to the sediment surface. All visible pneumatophores and burrow openings were counted by image analysis. The diameter of all detected crab burrows was measured digitally from the photographed sediment surfaces. The burrow inhabitants were not identified. Pneumatophore height was obtained from horizontal photos flush with the sediment surface at Olaria (n = 3) and Nobrega (n = 3). The height of all visible pneumatophores was measured by image analysis.

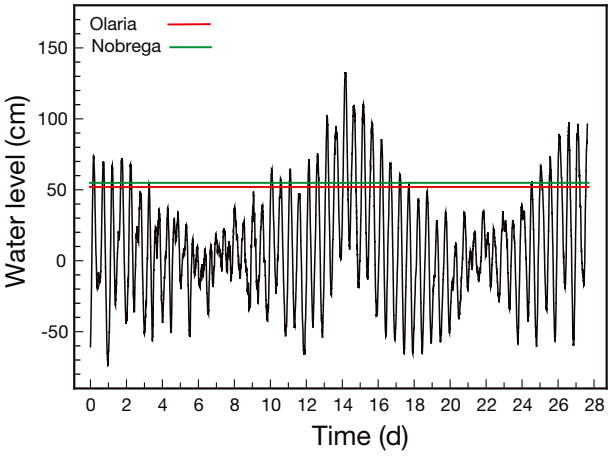

Fig. 2. Water level in Cananéia City, showing the tidal fluctuations during February 2014. The sediment surface level of the sampling sites at Olaria and Nobrega is shown by horizontal lines

2.3. Sediment characteristics

Sediment cores were collected from all sites by inserting core liners (30 cm long) into undisturbed sediment. The cores were dug out by hand and closed at both ends with rubber stoppers before transport to the laboratory at the University of São Paulo field station in Cananéia. Six sediment cores (20 cm deep, 5 cm inner diameter [i.d.]) were collected from each location for determination of solid phase granulometry and water content, as well as particulate organic carbon (POC), total nitrogen (TN) and surface sediment chlorophyll *a* (chl *a*) content.

Three sediment cores from each location were sectioned into 0–2, 4–6, 8–10 and 12–14 cm intervals. Sediment water content was determined from the weight loss after drying (60°C) subsamples to a constant weight. POC and TN were determined on dried samples with an elemental analyser (Flash EA 1112 Series, Thermo Finnigan) after acidification with HCl fumes to remove carbonates. Grain size distribution of other subsamples was analysed on a Malvern Mastersizer 3000 to obtain the median grain size and silt+clay content.

The upper 0.5 cm portions of 3 other sediment cores from each location were retained and immediately homogenized for chl *a* determination using the standard spectrophotometric method (Parsons et al. 1984). Subsamples of sediment were extracted overnight in 5 ml of 90% ethanol in darkness at 5°C. The extract was centrifuged at 1200 × *g*, and absorbance of the supernatant was measured at 665 and 750 nm before and after acidification with 2 drops of 1 M HCl.

2.4. *In situ* CO_2 and CH_4 exchange across the sediment–air interface

The exchange of CO_2 and CH_4 between air-exposed sediment and the atmosphere at both study locations was determined during low tide on the mangrove forest floor with and without pneumatophores or crab burrows.

The exchange of CO_2 was measured with a portable LI-COR 6400 Photosynthesis System equipped with a custom-made dynamic CO_2 flux chamber (18 cm long, 8 cm i.d.). Measurements were first conducted in light and darkness on bare sediment without pneumatophores and crab burrows. Three 10 cm long transparent acrylic core tubes with 8 cm i.d. were pushed about 5–7 cm into the sediment at each location. The tubes were left open for at least 30 min to equilibrate and thereafter sealed gas-tight using a rubber septum with the transparent LI-COR 6400 measuring chamber for light incubations. The LI-6400 was set for closed-chamber measurement, while the circulation pump in the sensor head assured a recirculating gas phase in the chamber. Exchange of CO_2 gas with the chamber in each position was measured for 3 × 5 min with CO_2 measurements every 10 s. Chamber CO_2 typically changed linearly during measurements. The chamber was lifted from the core tubes for 1 min between each 5 min measurement series to allow re-equilibration with the atmosphere.

Light intensity at the mangrove forest floor was determined continuously by a built-in quantum sensor in the LI-6400. Each core tube was then darkened with a bucket placed upside-down for 15–20 min to reset the enclosed sediment surface to dark conditions, and the measuring chamber was enclosed by an opaque plastic cap.

Exchange of CO_2 gas in darkness was then measured for 3 × 5 min on each core tube as described above. Subsequently, the dark measurements were repeated for 3 × 5 min with each of the 3 core tubes enclosing sediment with 1 average sized *A. schaueriana* pneumatophore. The procedure was repeated with each of the 3 core tubes placed on top of 1 average sized crab burrow. Rates of CO_2 exchange across the enclosed 50 cm^2 surface area were calculated based on the linear concentration change over time and volume of gas captured within the chambers.

Exchange of CH_4 was measured at both Olaria and Nobrega with static flux chambers consisting of 15 cm long acrylic core tubes (8 cm i.d.). Core tubes were pushed 5 cm into the sediment and sealed gas-tight at the top with rubber stoppers. Nine core tubes were deployed at each location with 3 in bare sediment, 3 enclosing 1 pneumatophore and 3 on top of 1 average-sized crab burrow. Sampling of the headspace gas was accomplished by 5 ml syringes connected to 2 hypodermic needles traversing the rubber stopper. Gas samples were retrieved from the headspace of each chamber. While samples of about 5 ml gas were taken after 0, 45–60 and 100–120 min from the headspace with 1 syringe, constant pressure was maintained by simultaneously injecting 5 ml atmospheric air each time with the other syringe. A 2 ml sample was transferred to a 3 ml evacuated glass Exetainer®. The Exetainer vials were stored cool until analysis on a gas chromatograph within 1 mo. Rates of CH_4 exchange across the enclosed 50 cm^2 surface area were calculated from the linear concentration change over time during incubation

and corrected for chamber volume and dilution during sampling.

2.5. DIC exchange during submersion

Three sediment cores (8 cm i.d.) from the mangrove forest floor at both study locations were used for determination of DIC exchange in light and darkness during inundation. Transparent core liners (30 cm long) were pushed into sediment without biogenic structures and carefully dug out by hand. The sediment cores were closed at both ends with rubber stoppers and transported to the laboratory located at the University of São Paulo field station in Cananéia.

After return to the laboratory, the headspace of sediment cores was gently filled with aerated creek water collected at Olaria and Nobrega Creeks during core sampling. The cores were equipped with a rotating magnet that was driven by a central stirring magnet and placed in a flow-through water bath kept at a constant temperature (29°C). The water bath was darkened with a black plastic sheet. Cores were left open in darkness to acclimatize for ~2 h before headspace water was sampled for DIC in 20 ml gas-tight glass vials. The cores were closed gas-tight with rubber stoppers and were left to incubate for 2–3 h before the rubber stoppers were removed and water from each core was sampled as described above. After the dark incubations, the headspace of each core was re-filled with aerated creek water and cores were left open to acclimatize for 1 h in ambient light before repeating the DIC exchange incubation in light with a transparent lid instead of the rubber seal. DIC was analysed immediately by potentiometric Gran titration (Talling 1973), and the exchange was calculated from the concentration change during incubations after correction for water volume and sediment surface area. Gross primary production (GPP) was calculated by subtracting dark rates from light rates.

3. RESULTS

3.1. Sediment environment and biogenic structures

Sediment granulometry and organic content showed no specific trends with depth in the upper 14 cm of the sediment and are presented in Table 1 as averages for the entire sediment column. The 2 fringe mangrove locations, Olaria and Nobrega, also did not differ significantly among most sediment characteristics. The sediment at both locations consisted roughly of 50% silt+clay with a median grain size of 57–65 µm (Table 1). POC and TN content was higher by 38% (*t*-test, $p < 0.01$) and 20% (*t*-test, $p < 0.05$), respectively, at Nobrega compared to Olaria. Chl *a* content in the upper 0.5 cm of the sediment was almost 2 times higher at Olaria than at Nobrega (*t*-test, $p < 0.001$) (Table 1).

Table 1. Sediment parameters at 2 study locations in Brazil (Olaria and Nobrega). Solid phase values are given as means (SD) from depth profiles down to 14 cm into the sediment (n = 3). Chlorophyll *a* is given as the mean (SD) of the 0–0.5 cm layer of 3 cores (n = 3). POC: particulate organic carbon; TN: total nitrogen; ww: wet weight; dw: dry weight

Parameter	Olaria	Nobrega
Median grain size (µm)	65 (13)	57 (23)
Silt+clay (%)	49.7 (4.4)	54.3 (8.1)
Water content (% ww)	63.3 (4.2)	66.5 (2.7)
POC (% dw)	5.0 (0.4)	6.9 (0.2)
TN (% dw)	0.34 (0.03)	0.40 (0.02)
POC:TN (mol)	17.4 (2.2)	20.0 (1.7)
Chl *a* (µg cm^{-3})	3.2 (0.1)	1.7 (0.1)

Pneumatophores and crab burrows were abundant on the mangrove forest floor at both locations with densities of 180–254 and 89–125 m^{-2}, respectively (Table 2). Although we found no significant differ-

Table 2. Density and size of *Avicennia schaueriana* pneumatophores and crab burrows on the forest floor in Olaria and Nobrega. For comparison, sizes are also given for pneumatophores and burrows enclosed within the CO_2 and CH_4 flux chambers. Pneumatophore size is given as height, while burrow size is indicated as the diameter of the opening at the sediment surface. Values are given as mean (SD)

	Olaria		Nobrega	
	Value	n	Value	n
***In situ* density (m^{-2})**				
Pneumatophore	253.7 (203.8)	14	180.2 (22.5)	9
Burrow	124.8 (51.1)	14	89.0 (31.1)	9
***In situ* size (cm)**				
Height of pneumatophore	8.1 (2.7)	59	8.4 (2.5)	48
Diameter of burrow opening	1.0 (1.0)	767	1.4 (1.6)	359
CO_2 chamber size (cm)				
Height of pneumatophore	9.5 (1.3)	3	8.2 (2.8)	3
Diameter of burrow opening	1.2 (0.2)	3	1.2 (0.1)	3
CH_4 chamber size (cm)				
Height of pneumatophore	5.2 (1.0)	3	6.7 (0.6)	3
Diameter of burrow opening	2.0 (0.5)	3	2.3 (0.3)	3

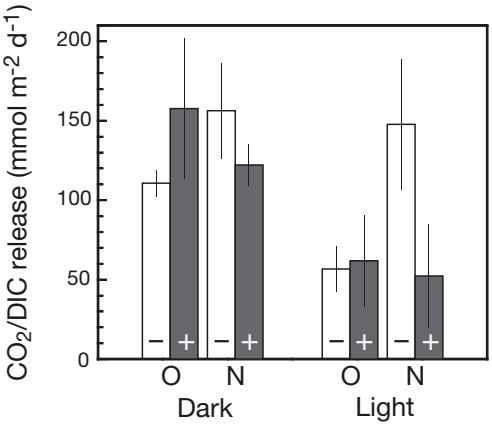

Fig. 3. CO_2 release from air-exposed ('–') and dissolved inorganic carbon release from inundated ('+') forest sediment without pneumatophores and crab burrows at 2 sites: Olaria (O) and Nobrega (N). Rates are given as means ± SE

ence between locations, high standard deviations point to a patchy distribution of these biogenic structures. At both locations, average pneumatophore height was slightly above 8 cm with a diameter of 0.5–1 cm, while the average diameter of burrow openings was 1–1.4 cm (Table 2).

3.2. Exchange of C gases during air exposure

In darkness, emission of CO_2 from air-exposed fringe mangrove sediments without biogenic structures (bare) ranged from 111 mmol m^{-2} d^{-1} at Olaria to a non-significantly higher level of 156 mmol m^{-2} d^{-1} at Nobrega (Fig. 3). The corresponding emissions during light exposure at the 2 locations were lower, 57 and 148 mmol m^{-2} d^{-1}, respectively, providing a wet season benthic GPP of 54 and 8 mmol m^{-2} d^{-1}, respectively. The light intensity at the mangrove forest floor during light incubations was (mean ± SD) 580 ± 133 mE m^{-2} s^{-1} at Olaria and 481 ± 445 µE m^{-2} s^{-1} at Nobrega. Since the impact of biogenic structures on CO_2 emission was measured with the 8 cm i.d. incubation chambers enclosing either 1 pneumatophore or 1 crab burrow, the reported emissions represent a sediment surface with 200 pneumatophores or burrows m^{-2}. The presence of pneumatophores increased the measured dark CO_2 emission significantly (*t*-test, $p < 0.05$) by 123% at Olaria and 113% at Nobrega (Fig. 4) compared with bare sediment. The corresponding increase of 91 and 49%, respectively, in the presence of burrows was significant

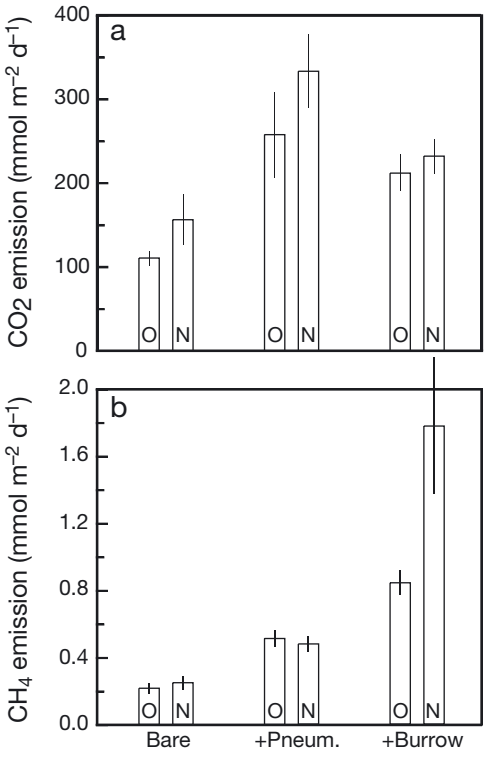

Fig. 4. Dark (a) CO_2 and (b) CH_4 emission at Olaria (O) and Nobrega (N) during air exposure. Fluxes were measured with chambers positioned over sediment devoid of biogenic structures (Bare), with 1 pneumatophore (+Pneum.) or with 1 crab burrow (+Burrow). The rates therefore represent a pneumatophore and burrow density of 200 m^{-2}, which is not the true density at the study sites (see Section 3.2 for details). Rates are given as mean ± SE (n = 3)

for Olaria (*t*-test, $p < 0.05$) and marginally significant for Nobrega (*t*-test, $p = 0.066$). Accordingly, each pneumatophore was estimated to emit 682 µmol CO_2 d^{-1} at Olaria and 887 µmol CO_2 d^{-1} at Nobrega (Table 3). Similarly, each burrow opening emitted 505 µmol CO_2 d^{-1} at Olaria and 381 µmol CO_2 d^{-1} at

Table 3. Contribution of individual pneumatophores and burrows to CO_2 and CH_4 emission during air exposure in darkness. The estimated total emission of mangrove forests in Olaria and Nobrega is given for the observed density of pneumatophores and burrows (Table 2). Values are mean (SD)

	Olaria		Nobrega	
	CO_2	CH_4	CO_2	CH_4
Individual emission (µmol ind.$^{-1}$ d^{-1})				
Pneumatophore	682 (522)	1.49 (0.50)	887 (458)	1.16 (0.52)
Burrow	505 (454)	3.15 (0.69)	381 (440)	7.65 (3.99)
Estimated total emission (mmol m^{-2} d^{-1})				
Forest floor with biogenic structures	347 (145)	0.99 (0.16)	350 (105)	1.14 (0.37)

Nobrega. By considering these individual rates and the observed average density of pneumatophores and burrow openings (Table 2), the total emission from air-exposed and darkened sediment at the 2 mangrove locations during the warm wet season was similar, around 350 mmol m^{-2} d^{-1} (Table 3).

Emission of CH_4 from air-exposed bare fringe mangrove sediments was 0.22–0.25 mmol m^{-2} d^{-1}, with no significant difference between locations. The measured CH_4 emission in the presence of 200 pneumatophores m^{-2} increased significantly (*t*-test, $p < 0.05$) by 137 % at Olaria and 92 % at Nobrega (Fig. 4). The corresponding significant (*t*-test, $p < 0.01$) increase in the measured CH_4 emission with 200 burrows m^{-2} present was much larger, reaching 288 % at Olaria and 607 % at Nobrega. This leads to individual emissions of 1.16–1.49 µmol CH_4 d^{-1} from pneumatophores and 3.15–7.65 µmol CH_4 d^{-1} from burrows (Table 3). When the observed average densities of these biogenic structures at Olaria and Nobrega are considered, the total CH_4 emission from air-exposed sediment was similar at the 2 locations in the warm wet season, with rates of 0.99–1.14 mmol m^{-2} d^{-1}.

3.3. Exchange of DIC during inundation

DIC release from darkened and inundated fringe mangrove sediments to the overlying water was 158 mmol m^{-2} d^{-1} in cores from Olaria, which was not significantly different from cores from Nobrega (122 mmol m^{-2} d^{-1}). Inundated cores from Olaria and Nobrega incubated in light showed a DIC release of 62 and 52 mmol m^{-2} d^{-1}, respectively. This leads to a potential warm wet season GPP of 96 and 70 mmol m^{-2} d^{-1}, respectively. It should be noted that these cores were exposed to light intensities of 1427 ± 285 µE m^{-2} s^{-1} during incubation, which was about 3 times higher than the irradiance recorded *in situ* under the mangrove canopy.

4. DISCUSSION

The 2 studied fringe mangrove locations in Brazil were similar with respect to sediment characteristics and C gas fluxes during the warm wet season despite the proximity of Olaria creek to potential anthropogenic impacts from Cananéia City (Barcellos et al. 2005). Others have reported that greenhouse gas emissions from mangrove sediments are increased substantially by anthropogenic nutrient and organic matter inputs (Chen et al. 2011, Zheng et al. 2018, Gnanamoorthy et al. 2022). The anthropogenic impact at Olaria must therefore be considered negligible at the time of our study, confirming the resilience of mangrove environments to moderate eutrophication (Kristensen & Suraswadi 2002, Kristensen et al. 2011, Penha-Lopes et al. 2012, Valiela et al. 2020). The present study demonstrates instead that a major controlling factor for CO_2 and CH_4 emissions from these mangrove sediments is the presence of biogenic structures, like pneumatophores and crab burrows. Consequently, C gas emissions across the sediment–air interface measured at sites where these structures are absent may seriously underestimate the true rates (Kitaya et al. 2002, Kristensen et al. 2008, Lin et al. 2021). It is therefore apparent that the contribution from pneumatophores and crab burrows must be included to fill an often-missing gap in mangrove C budgets (Kristensen et al. 2022).

The background emission of C gases from long-term air-exposed and darkened sediment devoid of pneumatophores and crab burrows at Olaria and Nobrega was 2–3 times higher than the global average compiled by Kristensen et al. (2022), but comparable to that reported for other mangrove sediments (Alongi et al. 2012). The high rates recorded in the present study must therefore be partly related to the lability of sediment organic matter at Olaria and Nobrega. Furthermore, it is known that CO_2 and CH_4 emissions from mangrove sediments driven by microbial degradation of deposited litter and allochthonous materials is strongly enhanced in locations like Olaria and Nobrega, which have long air-exposure time (Alongi et al. 2012, Chanda et al. 2014, Lin et al. 2021).

The increased emission of C gases from air-exposed sediment in the presence of pneumatophores and crab burrows at Olaria and Nobrega (Fig. 3) substantiates their potential for stimulation of organic matter degradation and importance as air-filled conduits for gas exchange. The contribution from individual biogenic structures to CO_2 emission (381–887 µmol ind.$^{-1}$ d^{-1}) is comparable between locations and type of biogenic structures, and similar to the rates of 207–678 µmol ind.$^{-1}$ d^{-1} reported by Kitaya et al. (2002), Kristensen et al. (2008) and Penha-Lopes et al. (2010). Emission of CH_4 from individual pneumatophores of ~1 µmol ind.$^{-1}$ d^{-1} at Olaria and Nobrega is comparable to rates reported by Kreuzwieser et al. (2003) and Kristensen et al. (2008). However, the 10–20 times higher individual CH_4 emissions from crab burrows at Olaria and Nobrega than reported previously (Kristensen et al. 2008, Penha-Lopes et al. 2010) are surprising and

may reflect extraordinarily extensive burrow networks and deep drainage during the long-term exposure at low tide at the 2 study locations.

Pneumatophores have numerous open lenticels during air exposure that allow for rapid diffusive exchange of gases between the air-filled aerenchyma tissue of roots and the atmosphere (Purnobasuki & Suzuki 2005). The CO_2 emitted from pneumatophores is partly derived from microbial C oxidation in sediments surrounding deep roots via transport across the root epidermis and partly from direct root respiration (Geissler et al. 2002, Kitaya et al. 2002, Lovelock et al. 2006). Drained crab burrows, on the other hand, augment gas exchange by providing a mosaic of deep subsurface sediment–air interfaces for rapid diffusive transport gases to and from the atmosphere. In this case, emitted CO_2 will originate from microbial action within the sediment and from respiration by the crab inhabitant (Datta 2005, Penha-Lopes et al. 2010, Tomotsune et al. 2020). Furthermore, common to both pneumatophores and crab burrows is their capacity to stimulate aerobic microbial degradation of organic matter in excess of the background anaerobic rates by their translocation of oxygen deep into the sediment (Nielsen et al. 2003, Kristensen 2008, Thomas & Blum 2010, Cheng et al. 2020). Conversely, emission of CH_4 from pneumatophores and burrows originates solely from methanogenesis in the surrounding anoxic sediment because plant roots and crabs residing inside burrows do not generate CH_4 (Kreuzwieser et al. 2003, Kristensen et al. 2008, Lin et al. 2021). Methanogenesis usually occurs deep in sediment where all electron acceptors (O_2, NO_3^-, Fe(III) and SO_4^{2-}) used for microbial heterotrophic respiration are depleted (Canfield et al. 2005). Substantial efflux of CH_4 from mangrove sediments therefore requires pneumatophores with aerenchyma tissue or drained crab burrows as deep air-filled conduits, because most of the generated CH_4 otherwise is oxidized before reaching the atmosphere when diffusing slowly upward within the sediment.

The role of biogenic structures for gas exchange during inundation is strongly hampered because lenticels of pneumatophores are closed and burrows typically are plugged by their inhabitants or filled with stagnant water (De la Iglesia et al. 1994, Skelton & Allaway 1996, Allaway et al. 2001). Transport of gases during inundation is therefore limited to diffusion within sediment porewater and at the sediment–water interface. Accordingly, the DIC release from darkened and inundated Olaria and Nobrega sediments is remarkably similar to the CO_2 emission from darkened and air-exposed bare sediment (Fig. 3). Unfortunately, there are no measurements of CH_4 release from inundated sediment in the present study, but previous studies have revealed that the vertical diffusion of CH_4 across the sediment–water interface it is very low in mangrove forests (Alongi et al. 2000, Kreuzwieser et al. 2003, He et al. 2019, Kristensen et al. 2022). Following inundation, release of CO_2 and CH_4 to mangrove waters and subsequent emission to the atmosphere may instead occur by tidal flushing and lateral drainage into creeks via crab burrows and other crevices during ebb tides (Call et al. 2019, Ohtsuka et al. 2020). Since this contribution was not considered in the present study, the emission budgets for Olaria and Nobrega (Table 4) are probably underestimated.

A preliminary carbon balance for fringe mangrove forests near Cananéia can be established using recently published litterfall and C sequestration

Table 4. Mean (SD) daily CO_2 and CH_4 emissions of mangrove forests in Olaria and Nobrega during February 2014. Rates are estimated from hourly dark and light emissions during air exposure and inundation. The contribution from pneumatophores and crab burrows is only included during air exposure. Dashes (–) indicate that CH_4 emission was not measured during inundation. The light rates during inundation are normalized to *in situ* light conditions. Calculations are based on the presented average daily inundation time and dark hours. DIC: dissolved inorganic carbon

	Olaria		Nobrega	
	Dark	Light	Dark	Light
CO_2 emission exposed (mmol m^{-2} h^{-1})	14.45 (6.03)	12.21 (6.09)	14.58 (4.38)	14.23 (4.83)
DIC release inundated (mmol m^{-2} h^{-1})	6.57 (3.19)	2.58 (1.20)	5.09 (0.93)	2.18 (1.35)
CH_4 emission exposed (µmol m^{-2} h^{-1})	41.21 (6.79)	41.21 (6.79)	47.53 (15.58)	47.53 (15.58)
CH_4 emission inundated (µmol m^{-2} h^{-1})	–	–	–	–
Daily average inundation time (h)	1.8	1.6	1.7	1.4
Dark hours per day	12	12	12	12
Mean daily CO_2 emission (mmol m^{-2})	290.0		312.8	
Mean daily CH_4 emission (µmol m^{-2})	848.9		993.4	

data. Rovai et al. (2021) measured litterfall to an equivalent of 30.9 ± 1.4 mol C m^{-2} yr^{-1}. This is an underestimate of the true mangrove tree net primary production (NPP) since the contribution from trunk (wood) and root growth is unaccounted for. The latter compartments are typically responsible for about ⅔ of the total tree NPP (Alongi 2020b). By correcting for this deficit, the Cananéia NPP estimate (92.6 mol C m^{-2} yr^{-1}) approaches that of the global average reported by Alongi (2020b).

The similarity in CO_2 release from Olaria and Nobrega sediments obtained in the present study indicates that the selected study sites are representative of the Cananéia fringe mangrove forest. With correction for inundation time, light/dark cycles and biogenic structures (Table 4), the CO_2 release measured during February in the warm wet season can be extrapolated to a net ecosystem loss of 8.70 and 9.38 mol C m^{-2} mo^{-1}, respectively. However, the fraction of CO_2 emission from pneumatophores that is derived from root respiration (i.e. ~30%, Ouyang et al. 2018) should not be considered a C sink, as it has already been accounted for in NPP calculations. By correcting for this, the estimated February CO_2 loss is reduced to 7.22 and 8.00 mol C m^{-2} mo^{-1}, respectively.

Since monthly average temperature in the Cananéia area ranges from ~28°C in February to ~20°C in July (Cunha-Lignon et al. 2009), an annual emission estimate can only be obtained by correcting sediment metabolism for this temperature difference. By applying a typical Q_{10} for sediment microbial processes of 2.5 (Thamdrup et al. 1998), the cold season (July) CO_2 loss at Olaria and Nobrega is 3.5 and 3.8 mol C m^{-2} mo^{-1}, leading to a full-year extrapolation of 64.1 and 71.0 mol C m^{-2} yr^{-1}. Accordingly, 28.5 and 21.6 mol C m^{-2} yr^{-1} of the above-mentioned NPP is not recycled, which is amazingly similar to the C accretion of 23.6 mol C m^{-2} yr^{-1} estimated by Rovai et al. (2021). This fringe forest estimate is somewhat higher than the net global mangrove C sequestration estimates of 8–17 mol C m^{-2} yr^{-1} reported previously (Alongi 2012, 2020b, Hutchison et al. 2014, Ouyang et al. 2017, Pérez et al. 2018, Jennerjahn 2020). It should be noted, however, that the present C budget does not consider import of allochthonous C and export of particulate and dissolved C to and from the Olaria and Nobrega mangrove forests. The values should therefore be considered rather crude and preliminary estimates. Nevertheless, if biogenic structures are not considered in the C budget, CO_2 emission at Olaria and Nobrega will be reduced by two-thirds, leading to a major C gap that cannot be explained only by the missing import and export.

The integrated total CH_4 emissions for Olaria and Nobrega mangrove forests, when rates from February 2014 (Table 4) are extrapolated to a full year after correcting for temperature dependence, is equivalent to a loss of 2.8–3.3 mol C m^{-2} yr^{-1} after conversion to C-units using the global warming potential of this gas. The CH_4 contribution driven by pneumatophores and crab burrows will therefore counteract the climate mitigation effect of the buried blue carbon by 10–15%. The important role of biogenic structures for emission of greenhouse gases other than CO_2 was also confirmed by Al-Haj & Fulweiler (2020) and Kristensen et al. (2022). They argued that emission of CH_4 and N_2O under the influence of these structures may completely expunge the climate effect of blue carbon in some mangrove forests. However, there are considerable uncertainties in the global mangrove climate budgets due to the large variability in NPP estimates, C sequestration, greenhouse gas emissions and tidal C export among forests. Some mangrove environments may have a large mitigation capacity, while others are neutral or even negative. More surveys at larger scales involving biogenic structures appropriately with high spatial and temporal resolution in various mangrove forest types at local, regional and global levels are therefore required to fully elucidate the climate mitigation capacity of these important ecosystems. Nevertheless, the present study emphasizes that C budgets will have serious gaps if the contribution of pneumatophores and crab burrows to greenhouse gas emissions is ignored.

Acknowledgements. We thank the technicians at the Dr. João de Paiva Carvalho field station, Instituto Oceanográfico of Universidade de São Paulo, for assistance during field sampling. The research was funded by the Danish Council for Independent Research (contract# 12-127012) to E.K.

LITERATURE CITED

Aidar E, Sigaut-Kutner TCS, Nishihara L, Schincke KP, Braga MCC, Farah RE, Kutner MBB (1997) Marine phytoplankton assays: effects of detergents. Mar Environ Res 43:55–68

Al-Haj AN, Fulweiler RW (2020) A synthesis of methane emissions from shallow vegetated coastal ecosystems. Glob Change Biol 26:2988–3005

Allaway WG, Curran M, Hollington LM, Ricketts MC, Skelton NJ (2001) Gas space and oxygen exchange in roots of *Avicennia marina* (Forssk.) Vierh. var. *australasica* (Walp.) Moldenke ex N. C. Duke, the grey mangrove. Wetlands Ecol Manag 9:221–228

Alongi DM (2012) Carbon sequestration in mangrove forests. Carbon Manag 3:313–322

Alongi DM (2020a) Carbon cycling in the World's mangrove ecosystems revisited: significance of non-steady state diagenesis and subsurface linkages between the forest floor and the coastal ocean. Forests 11:977

Alongi DM (2020b) Carbon balance in salt marsh and mangrove ecosystems: a global synthesis. J Mar Sci Eng 8: 767

Alongi DM, Tirendi F, Clough BF (2000) Below-ground decomposition of organic matter in forests of the mangroves *Rhizophora stylosa* and *Avicennia marina* along the arid coast of Western Australia. Aquat Bot 68:97–122

Alongi DM, de Carvalho NA, Amaral AL, da Costa A, Trott L, Tirendi F (2012) Uncoupled surface and below-ground soil respiration in mangroves: implications for estimates of dissolved inorganic carbon export. Biogeochemistry 109:151–162

Barcellos RL, Berbel GBB, Braga ES, Furtado VV (2005) Distribuição e características do fósforo sedimentary no sistema estuarino lagunar de Cananéia-Iguape, Estado de São Paulo, Brasil. Geochim Bras 19:22–36

Bouillon S, Borges AV, Castañeda-Moya E, Diele K and others (2008) Mangrove production and carbon sinks: a revision of global budget estimates. Global Biogeochem Cycles 22:GB2013

Call M, Santos IR, Dittmar T, de Rezende CE, Asp NE, Maher DT (2019) High pore-water derived CO_2 and CH_4 emissions from a macro-tidal mangrove creek in the Amazon region. Geochim Cosmochim Acta 247:106–120

Canfield DE, Kristensen E, Thamdrup B (2005) Aquatic geomicrobiology. Academic Press, San Diego, CA

Chanda A, Akhand A, Manna S, Dutta S and others (2014) Measuring daytime CO_2 fluxes from the inter-tidal mangrove soils of Indian Sundarbans. Environ Earth Sci 72: 417–427

Chen GC, Tam NFY, Wong YS, Ye Y (2011) Effect of wastewater discharge on greenhouse gas fluxes from mangrove soils. Atmos Environ 45:1110–1115

Cheng H, Liu Y, Jiang ZY, Wang YS (2020) Radial oxygen loss is correlated with nitrogen nutrition in mangroves. Tree Physiol 40:1548–1560

Cunha-Lignon M, Mahiques MM, Schaeffer-Novelli Y, Rodrigues M and others (2009) Analysis of mangrove forest succession, using sediment cores: a case study in the Cananeia-Iguape coastal system, Sao Paulo, Brazil. Braz J Oceanogr 57:161–174

Datta M (2005) Computer model for gas diffusion from nests of burrowing animals. Ethn Dis 15:62–63

de la Iglesia HO, Rodriguez EM, Dezi RE (1994) Burrow plugging in the fiddler crab *Uca uruguayensis* and its synchronization with two environmental cycles. Physiol Behav 55:913–919

Friess DA, Rogers K, Lovelock CE, Krauss KW and others (2019) The state of the World's mangrove forests: past, present, and future. Annu Rev Environ Resour 44:89–115

Geissler N, Schnetter R, Schnetter ML (2002) The pneumathodes of *Laguncularia racemosa*: little known rootlets of surprising structure, and notes on a new fluorescent dye for lipophilic substances. Plant Biol 4:729–739

Gillett NP, Matthews HD (2010) Accounting for carbon cycle feedbacks in a comparison of the global warming effects of greenhouse gases. Environ Res Lett 5:034011

Giri C, Ochieng E, Tieszen LL, Zhu Z and others (2011) Status and distribution of mangrove forests of the world using earth observation satellite data. Glob Ecol Biogeogr 20:154–159

Gnanamoorthy P, Chakraborty S, Nagarajan R, Ramasubramanian R and others (2022) Seasonal variation of methane fluxes in a mangrove ecosystem in South India: an eddy covariance-based approach. Estuaries Coasts 45:551–566

He Y, Guan W, Xue D, Liu L and others (2019) Comparison of methane emissions among invasive and native mangrove species in Dongzhaigang, Hainan Island. Sci Total Environ 697:133945

Hutchison J, Manica A, Swetnam R, Balmford A, Spalding M (2014) Predicting global patterns in mangrove forest biomass. Conserv Lett 7:233–240

Jennerjahn TC (2020) Relevance and magnitude of 'Blue Carbon' storage in mangrove sediments: carbon accumulation rates vs. stocks, sources vs. sinks. Estuar Coast Shelf Sci 247:107027

Kitaya Y, Yabuki K, Kiyota M, Tani A, Hirano T, Aiga I (2002) Gas exchange and oxygen concentration in pneumatophores and prop roots of four mangrove species. Trees (Berl) 16:155–158

Kreuzwieser J, Buchholz J, Rennenberg H (2003) Emission of methane and nitrous oxide by Australian mangrove ecosystems. Plant Biol 5:423–431

Kristensen E (2008) Mangrove crabs as ecosystem engineers, with emphasis on sediment processes. J Sea Res 59:30–43

Kristensen E, Suraswadi P (2002) Carbon, nitrogen and phosphorus dynamics in creek water of a Southeast Asian mangrove forest. Hydrobiologia 474:197–211

Kristensen E, Flindt MR, Ulomi S, Borges AV, Abril G, Bouillon S (2008) Emission of CO_2 and CH_4 to the atmosphere by sediments and open waters in two Tanzanian mangrove forests. Mar Ecol Prog Ser 370:53–67

Kristensen E, Mangion P, Tang M, Flindt MR, Ulomi S (2011) Benthic metabolism and partitioning of electron acceptors for microbial carbon oxidation in sediments of two Tanzanian mangrove forests. Biogeochemistry 103: 143–158

Kristensen E, Connolly RM, Otero XL, Marchand C, Ferreira TO, Rivera-Monroy VH (2017) Biogeochemical cycles: global approaches and perspectives. In: Rivera-Monroy VH, Lee SY, Kristensen E, Twilley RR (eds) Mangrove ecosystems: a global biogeographic perspective. Structure, function and ecosystem services. Springer Nature, Cham, p 169–209

Kristensen E, Quintana CO, Petersen SGG (2022) The role of biogenic structures for greenhouse gas balance in vegetated intertidal wetlands. In: Ouyang X, Lee SY, Lai YFD, Marchand C (eds) Carbon mineralization in coastal wetlands: from litter decomposition to greenhouse gas dynamics. Elsevier, Amsterdam, p 233–267

Lin CW, Kao YC, Lin WJ, Ho CW, Lin HJ (2021) Effects of pneumatophore density on methane emissions in mangroves. Forests 12:314

Lovelock CE, Ruess RW, Feller IC (2006) Fine root respiration in the mangrove *Rhizophora mangle* over variation in forest stature and nutrient availability. Tree Physiol 26: 1601–1606

Macreadie PI, Costa MDP, Atwood TB, Friess DA and others (2021) Blue carbon as a natural climate solution. Nat Rev Earth Environ 2:826–839

Matos CRL, Berrêdo JF, Machado W, Sanders CJ, Metzger E, Cohen MCL (2020) Carbon and nutrient accumulation in tropical mangrove creeks, Amazon region. Mar Geol 429:106317

Myhre G, Shindell D, Bréon FM, Collins W and others (2013) Anthropogenic and natural radiative forcing. In: Stocker TF, Qin D, Plattner GK, Tignor M and others (eds) Climate change 2013: the physical science basis. Contribution of Working Group I to the Fifth Assessment Report of the Intergovernmental Panel on Climate Change. Cambridge University Press, Cambridge, p 659–740

Nielsen OI, Kristensen E, Macintosh DJ (2003) Impact of fiddler crabs (*Uca* spp.) on rates and pathways of benthic mineralization in deposited mangrove shrimp pond waste. J Exp Mar Biol Ecol 289:59–81

Ohtsuka T, Onishi T, Yoshitake S, Tomotsune M and others (2020) Lateral export of dissolved inorganic and organic carbon from a small mangrove estuary with tidal fluctuation. Forests 11:1041

Ouyang X, Lee SY, Connolly RM (2017) The role of root decomposition in global mangrove and saltmarsh carbon budgets. Earth Sci Rev 166:53–63

Ouyang X, Lee SY, Connolly RM (2018) Using isotope labeling to partition sources of CO_2 efflux in newly established mangrove seedlings. Limnol Oceanogr 63: 731–740

Parsons TR, Maita Y, Lalli CM (1984) A manual of chemical and biological methods for seawater analysis. Pergamon Press, Oxford

Penha-Lopes G, Kristensen E, Flindt M, Mangion P, Bouillon S, Paula J (2010) The role of biogenic structures on the biogeochemical functioning of mangrove constructed wetlands sediments — a mesocosm approach. Mar Pollut Bull 60:560–572

Penha-Lopes G, Flindt MR, Ommen B, Kristensen E, Garret P, Paula J (2012) Organic carbon dynamics in a constructed mangrove wastewater wetland populated with benthic fauna: a modelling approach. Ecol Model 232: 97–108

Pérez A, Libardoni BG, Sanders CJ (2018) Factors influencing organic carbon accumulation in mangrove ecosystems. Biol Lett 14:20180237

Purnobasuki H, Suzuki M (2005) Aerenchyma tissue development and gas-pathway structure in root of *Avicennia marina* (Forsk.) Vierh. J Plant Res 118:285–294

Rosentreter JA, Al-Haj AN, Fulweiler RW, Williamson P (2021) Methane and nitrous oxide emissions complicate coastal blue carbon assessments. Global Biogeochem Cycles 35:e2020GB006858

Rovai AS, Coelho C Jr, de Almeida R, Cunha-Lignon M and others (2021) Ecosystem-level carbon stocks and sequestration rates in mangroves in the Cananéia-Iguape lagoon estuarine system, southeastern Brazil. For Ecol Manag 479:118553

Sasmito SD, Kuzyakov Y, Lubis AA, Murdiyarso D and others (2020) Organic carbon burial and sources in soils of coastal mudflat and mangrove ecosystems. CATENA 187:104414

Schaeffer-Novelli Y, Cintron-Molero G, Adaime RR, de Camargo TM (1990) Variability of mangrove ecosystems along the Brazilian coast. Estuaries 13:204–218

Schaeffer-Novelli Y, Soriano-Sierra EJ, do Vale CC, Bernini E and others (2016) Climate changes in mangrove forests and salt marshes. Braz J Oceanogr 64:37–52

Skelton NJ, Allaway WG (1996) Oxygen and pressure changes measured *in situ* during flooding in roots of the grey mangrove *Avicennia marina* (Forssk.) Vierh. Aquat Bot 54:165–175

Spalding EA, Kainuma M, Collins L (2011) World atlas of mangroves. ITTO, Kuala Lumpur

Talling JF (1973) The application of some electrochemical methods to the measurement of photosynthesis and respiration in fresh water. Freshw Biol 3:335–362

Thamdrup B, Hansen JW, Jørgensen BB (1998) Temperature dependence of aerobic respiration in a coastal sediment. FEMS Microbiol Ecol 25:189–200

Thomas CR, Blum LK (2010) Importance of the fiddler crab *Uca pugnax* to salt marsh soil organic matter accumulation. Mar Ecol Prog Ser 414:167–177

Tomotsune M, Arai H, Yoshitake S, Kida M, Fujitake N, Kinjo K, Ohtsuka T (2020) Effect of crab burrows on CO_2 flux from the sediment surface to the atmosphere in a subtropical mangrove forest on Ishigaki Island, southwestern Japan. Estuaries Coasts 43:102–110

Valiela I, Juman R, Asmath H, Hanacek D and others (2020) Water quality, nutrients, and stable isotopic signatures of particulates and vegetation in a mangrove ecosystem exposed to past anthropogenic perturbations. Reg Stud Mar Sci 35:101208

Wang F, Sanders CJ, Santos IR, Tang J and others (2021) Global blue carbon accumulation in tidal wetlands increases with climate change. Natl Sci Rev 8:nwaa296

Zheng X, Guo J, Song W, Feng J, Lin G (2018) Methane emission from mangrove wetland soils is marginal but can be stimulated significantly by anthropogenic activities. Forests 9:738

Editorial responsibility: Simon Pittman, Oxford, UK
Reviewed by: D. M. Alongi, F. Adame, J. B. Gallagher

Submitted: April 22, 2022
Accepted: August 2, 2022
Proofs received from author(s): September 16, 2022